Internal fracture of notched epoxy resins

I. Narisawa, T. Murayama and H. Ogawa
Department of Fiber and Polymer Engineering, Faculty of Engineering, Yamagata University, Yonezawa 992, *Japan*
(*Received* 2 *December* 1980; *revised* 11 *April* 1981)

The brittle fracture of round-notched epoxy resin bars subjected to plane strain bending has been studied at varying strain rates. Observations of fracture processes and surface morphologies revealed that the internal crack was nucleated at the plastic–elastic boundary when the plastic deformation zone at the notch root reached a certain size. A slip-line field theory allows calculation of the stress components at the plastic–elastic boundary from a knowledge of the location of the internal crack. An analysis of the data concluded that the triaxial stress level ahead of the plastic zone was raised by plastic constraints to an ideal fracture stress which is considerably larger than that of glassy thermoplastics.

Keywords Analysis; stress; strain; fracture; deformation; morphology; epoxy resins

INTRODUCTION

The mechanical criterion for fracture in thermosetting resins has been extensively investigated. The fracture mechanism of epoxy resins has received particular attention because of their use in structural engineering as adhesives and matrices for composite materials[1-3].

Although epoxy resins are known to be essentially brittle, they can exhibit some plastic deformation under certain circumstances[4]. Furthermore, the addition of a plasticizing agent allows a considerable amount of plastic deformation. For a material which shows plastic deformation prior to fracture under plane strain, and for which yielding occurs at the notch tip, the elastic material outside the yielding region provides a constraint to this region and the triaxial stress state is introduced by the constraint at the elastic–plastic boundary in the material. In certain glassy thermoplastics such as poly(methyl methacrylate), polycarbonate and poly(vinyl chloride), a dilatational stress produced by the stress triaxiality at the elastic–plastic boundary is largely responsible for craze and fracture initiation[5,6].

Except for the work of Kinloch and Williams[7], who investigated the crack tip blunting mechanism associated with shear yield in the stick–slip fracture of epoxy resins, there are no reports in the literature on this type of fracture mechanism in epoxy materials. Here, we extend the glassy thermoplastic results to crazing and fracture of notched specimens of epoxy resins subjected to plane strain bending and provide more experimental evidence of the dilatational fracture mechanism in thermosetting resins.

EXPERIMENTAL

Materials and specimen preparation

Materials used were a commercial diglycidyl ether of bisphenol A type resins, Epikote 828 (Shell) and a dimer acid type resin, Epikote 871 (Shell), frequently used to modify resin stiffness. Epikure Z (mixed aromatic amines) was used as a curing agent.

The stirred mixture of the resins and curing agent was degassed for 30 min before casting into plates. The mould essentially consisted of a cardboard gasket, 10 mm thick, clamped between glass plates, $180 \times 120 \times 1.3$ mm, lined with a sheet of cellophane 20 μm thickness. Material formulations and the curing schedule are listed in *Table 1*. *Figure 1* shows test specimens with a round notch in the centre of one edge, shaped by machining from the moulded plates. A round notch of 0.5 mm radius and 3.0 mm long was introduced by a saw cut. The notch root was polished by hand to prevent surface cracks, using wet billiard cloth with a polishing solution of Cr_2O_3.

Procedure

Specimens were loaded by three-point-bending with an Instron testing machine (Auto Graph, Shimazu DSS-5000) at varying crosshead speeds. The shear stress for yielding was obtained by plane strain compression tests

Table 1 Material formulation (by wt) and curing schedule

Material and curing	Sample A	Sample B	Sample C
Epikote 828	100	90	80
Epikote 871	0	10	20
Epkure Z	20	20	20
Initial cure	373K,	1 h	
After cure	423K,	4 h	

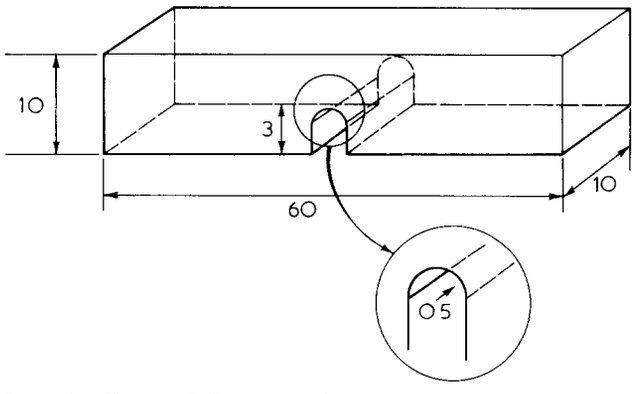

Figure 1 Shape and dimensions of test specimens

0032-3861/82/020291-04$03.00

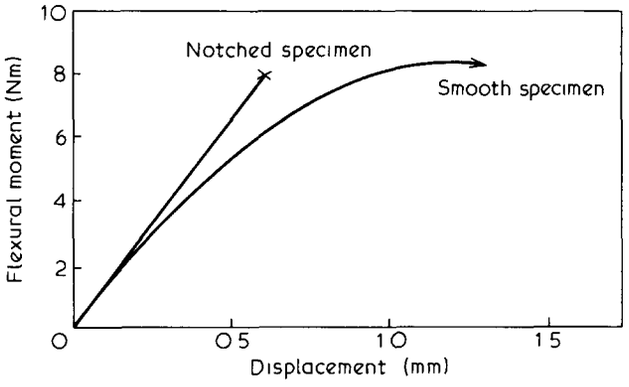

Figure 2 Comparison of flexural moment–displacement curves of notched specimen with that for a smooth specimen, sample A

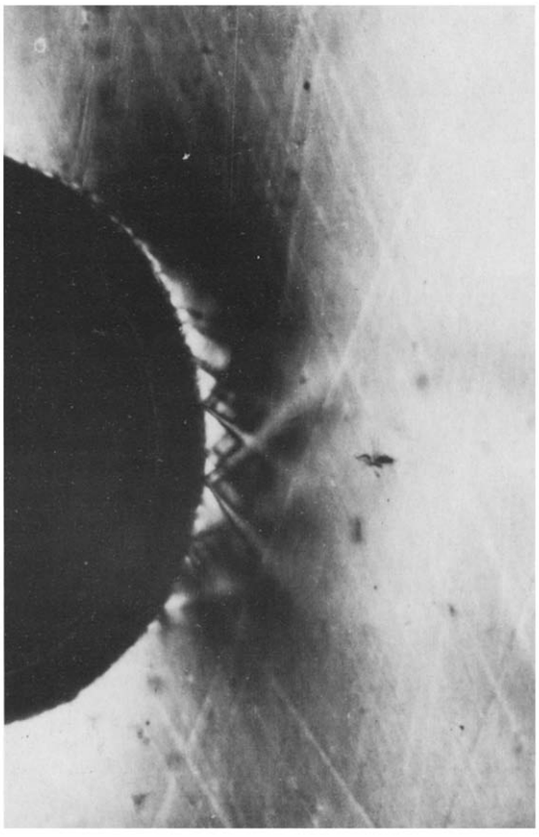

Figure 3 Polarized micrograph of a thin slice at midsection of the plastic zone, sample A

on the same specimens at varying crosshead speeds corresponding to the bending rates. Rectangular specimens 40 mm long, 10 mm wide and 2 mm thick were compressed between the 5 mm dies using the Auto Graph. All tests were made in air at 293K and 65% relative humidity. Optical and scanning electron microscopic observations were made on specimens unloaded during deformation and after fracture to examine the plastic deformation region and to determine the origin of fracture.

RESULTS

Plastic deformation and fracture processes

Figure 2 shows typical flexural moment–displacement curves for smooth and notched specimens of sample A at a crosshead speed of 1.0 mm/min. Polarized microscope examinations of the notched specimens unloaded stepwise during deformation revealed that plastic deformation initiated around the notch root at a moment 0.5 to 0.6 of the fracture moment. As the applied moment was increased, the plastic deformation spread from the notched root and, when the zone reached a certain size, the internal crack was initiated ahead of the plastic zone at an applied moment slightly below the fracture moment. As the applied moment was further increased, the internal crack grew and, eventually, brittle fracture occurred. The growth of the internal crack was so rapid that it was impossible to control the applied moment to observe it. Fracture moment decreased slightly with decreasing bending rate. Polarized microscope observations of a thin longitudinal slice at midsection showed that the plastic region consisted of broad shear bands as shown in *Figure 3*. These shear bands became obscure with increasing amounts of the plasticizing resin (samples B and C) but the fracture processes are in close agreement with those for sample A.

Fracture surfaces

A scanning electron microphotograph of the fracture surface of sample A is shown as an example in *Figure 4*. A comparatively smooth region in which the fracture originated can be clearly discerned. As shown in *Figure 5*,

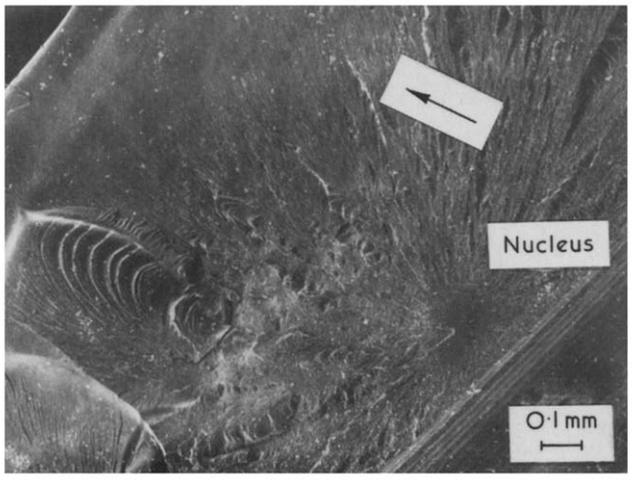

Figure 4 Scanning electron micrograph of fracture surface of sample A. Arrow indicates crack propagation direction

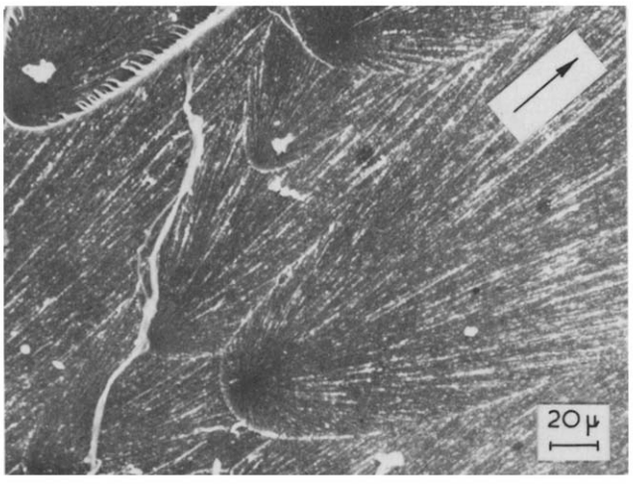

Figure 5 Parabolic marks around the smooth region. Arrow indicates crack propagation direction

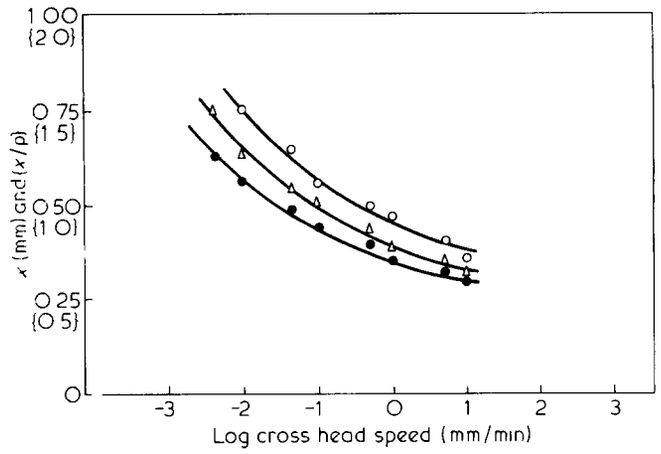

Figure 6 Variation of the maximum extent of the plastic zone x and the ratio of x to notch radius ρ. ○, Sample A; △, sample B; and ●, sample C

parabolas, can be occasionally observed around the fracture nucleus in the smooth region as observed for poly(methyl methacrylate). These parabolas indicate the direction of crack propagation.

Outside the smooth region across the width of the specimen the fracture surface is quite rough and there are many irregular lines which propagate radially across the smooth region. Although these fracture surface morphologies are significantly different from those reported by others[1,2], who observed smooth and relatively featureless fracture surfaces during fast crack propagation, this fracture surface has been observed to change with type and amount of curing agent, curing conditions and type of loading[2]. Similar fracture surfaces were observed in samples B and C.

Critical stress for fracture

Since the general characteristics of the fracture surfaces are quite similar to those of glassy thermoplastics, the fracture originates at the tip of the plastic deformation region. This means that the initiation of a crack nucleus is closely associated with the stress concentration caused by plastic constraints because of local plastic deformation at the notch root. In other words, the effect of plastic constraint raises the stress locally to that required for the initiation of the fracture.

When a rigid perfectly plastic body is assumed, the slip line field theory developed by Hill[8] can be applied to calculate the stress distribution in the plastic region. The theory shows that the plastic zone with a deep circular notch in plane strain, bending occurs in logarithmic spirals. The maximum stress, σ_y, along the axial direction of the specimen, within the logarithmic spiral region at a distance x ahead of the notch root is given by:

$$\sigma_y = 2k\{1+\ln(1+x/\rho)\} \tag{1}$$

where ρ is the notch radius and k is the shear stress for yield. The Tresca yield criterion satisfies the equation:

$$\sigma_y - \sigma_x = 2k \tag{2}$$

where σ_x is the stress component in the notch direction. If Poisson's ratio is 0.5, the stress component in the thickness direction, σ_z, can be written:

$$\sigma_z = \frac{1}{2}(\sigma_x + \sigma_y) \tag{3}$$

The triaxial hydrostatic stress is given by:

$$S = \frac{1}{3}(\sigma_x + \sigma_y + \sigma_z) \tag{4}$$

Substituting equations (1), (2) and (3) into (4), S can be expressed as:

$$S = \sigma_y - k = k\{1+2\ln(1+x/\rho)\} \tag{5}$$

However, the majority of polymers are not rigid perfectly plastic but elastic–plastic materials which generally show strain hardening after yield. In a previous paper[9], the results of stress distribution in the plastic zone ahead of the notch obtained from the slip line field theory have been compared with those obtained from finite element analysis, assuming an elastic–plastic, linearly strain-hardening material. The analysis reveals that the estimation of stress distribution from rigid perfectly plastic theory can be safely applied to glassy polymers.

Figure 6 shows the variation of the maximum extent of the plastic zone size x at fracture, and the ratio of x to the radius of the notch with bending rate. The plastic zone size of each sample decreases with increasing bending rate. Using equation (5), the critical stress for internal cracking at the elastic–plastic boundary can be calculated from the maximum extent of the plastic zone. It will be expressed as the ratio of the triaxial hydrostatic stress S to the shear yield stress k. In *Figure 7* the variation of the ratio S/k with the log-(crosshead speed) is shown. The shear yield stresses were calculated from the plane strain compressive yield stress σ_y using the relation $k = \sigma_y/2$. The compressive strain rates were selected so that yielding occurred on the same time scale in bending tests. *Figure 8* shows the variation of the critical hydrostatic stress for fracture and critical shear yield stress with the log (crosshead speed). Shear yield stresses are replotted against the crosshead speeds used for the bending tests. The shear yield stresses for the three samples increase, as usual, with crosshead

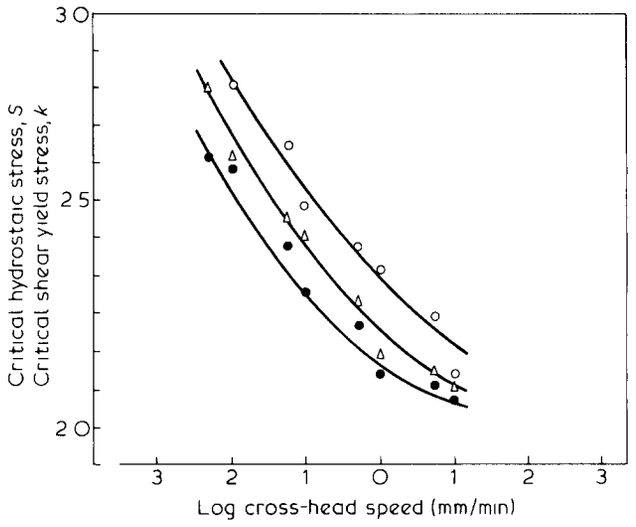

Figure 7 Variation of the ratio of the critical hydrostatic stress S to the shear yield stress k with the log (crosshead speed). ○, Sample A; △, sample B; and ●, sample C

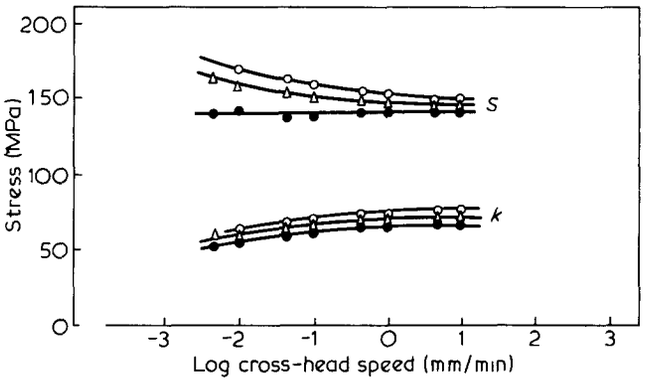

Figure 8 Variation of the critical hydrostatic stress S and shear yield stress k with the logarithm of crosshead speed. ○, Sample A; △, sample B; and ●, sample C

Table 2 Critical hydrostatic stress for internal fracture for epoxy resins and glassy thermoplastics at a crosshead speed of 0.5 mm min^{-1}

Polymer	S (MPa)
Polystyrene (slow cooled)	37
Polystyrene (quenched)	40
Acrylonitrile–styrene copolymer (slow cooled)	56
Acrylonitrile–styrene copolymer (quenched)	69
Poly(methyl methacrylate) (quenched)	74
Poly(vinyl chloride) (quenched)	67
Polycarbonate (slowly cooled)	87
Polycarbonate (quenched)	96
Epoxy, sample A	154
Epoxy, sample B	153
Epoxy, sample C	134

speed, but the critical hydrostatic stresses except for sample C shows a slight fall with increasing bending rate.

DISCUSSION AND CONCLUSIONS

The fracture processes and surface morphologies of these epoxy resins are quite similar to those of glassy thermoplastics under the same loading. In glassy thermoplastics such as polycarbonate, poly(methyl methacrylate) and poly(vinyl chloride), refractive index measurements showed that the internal crack nucleated at the elastic–plastic boundary is a craze which subsequently converts into an unstable crack with increasing load. However, there is little evidence for craze nucleation in epoxy resins except for the few limited observations of Lilley and Holloway[10], and Morgan and O'Neal[11]. In this experiment, since it was impossible to obtain unbroken epoxy samples containing the internal crack, we have been unable to determine whether the internal crack is a true crack or craze. However, analysis of experimental results on yielding and fracture processes under plane strain leads to the conclusion that fracture of epoxy resins, if they contain a deep notch, occurs when the stress level ahead of the plastic zone is raised by a plastic constraint to an ideal fracture stress which is comparatively larger than that of glassy thermoplastics (*Table 2*)[5,6,12].

REFERENCES

1 Philips, D. C., Scott, J. M. and Jones, M. *J. Mater. Sci.* 1978, **13**, 311
2 Yamini, S. and Young, R. J. *J. Mater. Sci.* 1979, **14**, 1609
3 Scott, J. M., Wells, G. M. and Phillips, D. C. *J. Mater. Sci.* 1980, **15**, 1436
4 Yamini, S. and Young, R. J. *J. Mater. Sci.* 1980, **15**, 1814
5 Ishikawa, M., Narisawa, I. and Ogawa, H. *J. Polym. Sci (Polym. Phys. Edn.)* 1977, **15**, 1791
6 Narisawa, I., Ishikawa, M. and Ogawa, H. *J. Mater. Sci.* 1980, **15**, 2059
7 Kinloch, A. J. and Williams, J. G. *J. Mater. Sci.* 1980, **15**, 987
8 Hill, R. 'Mathematical Theory of Plasticity', Oxford University Press, London, 1950
9 Ishikawa, M., Ogawa, H. and Narisawa, I. *J. Macromol. Sci. (B)*, 1981, **19**, 42
10 Lilley, J. and Holloway, D. G. *Phil. Mag.* 1973, **28**, 215
11 Morgan, R. J. and O'Neal, J. E. *J. Mater. Sci.* 1977, **12**, 1966
12 Narisawa, I., Ishikawa, M. and Ogawa, H. *Phil. Mag. (A)* 1980, **41**, 331